

# Cu(II) immobilized on guanidinated epibromohydrin-functionalized $\gamma\text{-Fe}_2\text{O}_3@TiO_2$ ( $\gamma\text{-Fe}_2\text{O}_3@TiO_2\text{-EG-Cu(II)}$ ): A highly efficient magnetically separable heterogeneous nanocatalyst for one-pot synthesis of highly substituted imidazoles

Mahdi Nejatianfar | Batool Akhlaghinia  | Roya Jahanshahi

Department of Chemistry, Faculty of Sciences, Ferdowsi University of Mashhad, Mashhad 9177948974, Iran

## Correspondence

Batool Akhlaghinia, Department of Chemistry, Faculty of Sciences, Ferdowsi University of Mashhad, Mashhad 9177948974, Iran.  
Email: akhlaghinia@um.ac.ir

A simple, efficient and eco-friendly procedure has been developed using Cu(II) immobilized on guanidinated epibromohydrin-functionalized  $\gamma\text{-Fe}_2\text{O}_3@TiO_2$  ( $\gamma\text{-Fe}_2\text{O}_3@TiO_2\text{-EG-Cu(II)}$ ) for the synthesis of 2,4,5-trisubstituted and 1,2,4,5-tetrasubstituted imidazoles, *via* the condensation reactions of various aldehydes with benzil and ammonium acetate or ammonium acetate and amines, under solvent-free conditions. High-resolution transmission electron microscopy analysis of this catalyst clearly affirmed the formation of a  $\gamma\text{-Fe}_2\text{O}_3$  core and a  $TiO_2$  shell, with mean sizes of about 10–20 and 5–10 nm, respectively. These data were in very good agreement with X-ray crystallographic measurements (13 and 7 nm). Moreover, magnetization measurements revealed that both  $\gamma\text{-Fe}_2\text{O}_3@TiO_2$  and  $\gamma\text{-Fe}_2\text{O}_3@TiO_2\text{-EG-Cu(II)}$  had superparamagnetic behaviour with saturation magnetization of 23.79 and 22.12 emu  $g^{-1}$ , respectively.  $\gamma\text{-Fe}_2\text{O}_3@TiO_2\text{-EG-Cu(II)}$  was found to be a green and highly efficient nanocatalyst, which could be easily handled, recovered and reused several times without significant loss of its activity. The scope of the presented methodology is quite broad; a variety of aldehydes as well as amines have been shown to be viable substrates. A mechanism for the cyclocondensation reaction has also been proposed.

## KEYWORDS

Cu(II) immobilized on guanidinated epibromohydrin-functionalized  $\gamma\text{-Fe}_2\text{O}_3@TiO_2$  ( $\gamma\text{-Fe}_2\text{O}_3@TiO_2\text{-EG-Cu(II)}$ ), heterogeneous nanocatalyst, solvent-free, substituted imidazoles

## 1 | INTRODUCTION

Imidazole ring-containing compounds, which are a subset of nitrogen-containing heterocyclic compounds, exhibit wide ranges of biological and pharmacological activities that make them very attractive compounds for organic chemists.<sup>[1,2]</sup> Many substituted imidazoles are known as biocides (in particular, herbicides, fungicides and growth regulators),<sup>[3]</sup> potent angiotensin II receptor

antagonists,<sup>[4]</sup> glucagon receptor antagonists<sup>[5]</sup> and inhibitors of interleukin-1 and 5-lipoxygenase.<sup>[6]</sup> Using imidazoles in ionic liquids<sup>[7]</sup> and in N-heterocyclic carbenes<sup>[8]</sup> has given a new dimension to the area of organometallics and 'green chemistry'. Also, imidazole derivatives have been used in photography as photosensitive compounds<sup>[9]</sup> and also as useful building blocks for the synthesis of other classes of compounds. Therefore, the development of novel synthetic methods towards the preparation of

substituted imidazoles has become an important target in recent years.

The traditional approaches for the preparation of both 2,4,5-trisubstituted and 1,2,4,5-tetrasubstituted imidazoles are mainly based on the cyclocondensation reaction of a 1,2-diketone with an aldehyde and a nitrogen source (ammonium acetate or ammonium acetate and amine).<sup>[10]</sup> Literature survey reveals that a great variety of catalysts, promoters and solvents have been developed for the synthesis of both 2,4,5-trisubstituted and 1,2,4,5-tetrasubstituted imidazoles, including the use of *n*-PeFBA,<sup>[11]</sup> HClO<sub>4</sub>-SiO<sub>2</sub>,<sup>[12]</sup> zeolite HY,<sup>[13]</sup> WD/SiO<sub>2</sub>,<sup>[14]</sup> RFOH/SBA-15-Pr-SO<sub>3</sub>H,<sup>[15]</sup> SZ,<sup>[16]</sup> Fe<sub>3</sub>O<sub>4</sub>,<sup>[17]</sup> Fe<sub>3</sub>O<sub>4</sub>-PEG-Cu,<sup>[18]</sup> InCl<sub>3</sub>·3H<sub>2</sub>O,<sup>[19]</sup> NiCl<sub>2</sub>·6H<sub>2</sub>O,<sup>[20]</sup> K<sub>5</sub>CoW<sub>12</sub>O<sub>40</sub>·3H<sub>2</sub>O,<sup>[21]</sup> silica gel/NaHSO<sub>4</sub>,<sup>[22]</sup> molecular iodine,<sup>[23]</sup> heteropolyacids,<sup>[24]</sup> MW/Al<sub>2</sub>O<sub>3</sub>,<sup>[25]</sup> trichloroiodoacetic acid,<sup>[26]</sup> benzotriazole,<sup>[27]</sup> ZrCl<sub>4</sub>,<sup>[28]</sup> acetic acid,<sup>[29]</sup> silica-supported sulfuric acid,<sup>[30]</sup> CAN,<sup>[31]</sup> Cu(TFA)<sub>2</sub>,<sup>[32]</sup> Yb(OTf)<sub>3</sub>,<sup>[33]</sup> GO-chitosan,<sup>[34]</sup> DABCO,<sup>[35]</sup> FeCl<sub>3</sub>·6H<sub>2</sub>O,<sup>[36]</sup> mercaptopropylsilica,<sup>[37]</sup> L-proline,<sup>[38]</sup> MCM-41 or *p*-TsOH,<sup>[39]</sup> and 1-butyl-3-methylimidazolium bromide.<sup>[40]</sup> Despite the many methods available for the synthesis of 2,4,5-trisubstituted and 1,2,4,5-tetrasubstituted imidazoles, most of these procedures suffer from one or more serious drawbacks such as use of expensive and hazardous acid catalysts, using toxic metal catalysts, harsh reaction conditions, occurrence of side reactions, laborious and complex work-up and purification, high temperature, long reaction time, low yields and using expensive and excess reagents. Therefore, the development of a new, green, high-yielding, mild and efficient catalytic system to overcome these shortcomings along with introducing a mild, efficient and environmentally benign protocol for the synthesis of highly substituted imidazoles is an important task in the planning of substituted imidazole synthesis.

In continuation of our efforts to explore the catalytic activity of heterogeneous Lewis and Brønsted acids<sup>[41]</sup> for various organic transformations, we report herein a simple, mild and expeditious synthesis of 2,4,5-trisubstituted and 1,2,4,5-tetrasubstituted imidazoles in high yields, using Cu(II) immobilized on guanidinated epibromohydrin-functionalized  $\gamma$ -Fe<sub>2</sub>O<sub>3</sub>@TiO<sub>2</sub> ( $\gamma$ -Fe<sub>2</sub>O<sub>3</sub>@TiO<sub>2</sub>-EG-Cu(II)) as an effectual catalyst.

## 2 | EXPERIMENTAL

### 2.1 | General

All chemical reagents and solvents were purchased from Merck and Sigma-Aldrich and were used as received without further purification. The purity

determinations of the products and the progress of the reactions were accomplished by TLC on silica gel polygram STL G/UV 254 plates. Melting points of the products were determined with an Electrothermal Type 9100 melting point apparatus. Fourier transform infrared (FT-IR) spectra were recorded with pressed KBr pellets using an AVATAR 370 FT-IR spectrometer (Thermo Nicolet, USA) at room temperature in the range 400–4000 cm<sup>-1</sup>, with a resolution of 4 cm<sup>-1</sup>, and each spectrum was the average of 32 scans. NMR spectra were obtained with a Bruker Avance NMR spectrometer at 300 MHz, using CDCl<sub>3</sub> and DMSO-*d*<sub>6</sub> solvents in the presence of tetramethylsilane as the internal standard. Elemental analyses were performed using a Thermo Finnigan Flash EA 1112 Series instrument (furnace: 900 °C; oven: 65 °C; flow carrier: 140 ml min<sup>-1</sup>; flow reference: 100 ml min<sup>-1</sup>). Mass spectra were recorded with a CH7A Varianmat Bremem instrument at 70 eV with electron impact ionization. Thermogravimetric analysis (TGA) and differential thermogravimetry (DTG) were carried out using a Shimadzu TG-50 thermogravimetric analyser in the temperature range 25–900 °C at a heating rate of 10 °C min<sup>-1</sup>, under air atmosphere. High-resolution transmission electron microscopy (HRTEM) was performed using a Philips CM30 microscope. Inductively coupled plasma (ICP) analysis was conducted with a VISTA-PRO, CCD (Varian, Australia). Elemental compositions were determined using energy-dispersive spectroscopy (EDS; SC7620) with a 133 eV resolution at 20 kV. Room temperature magnetization isotherms were obtained using vibrating sample magnetometry (VSM; LakeShore 7400). Powder X-ray diffraction (XRD) was performed using an X'Pert Pro MPD diffractometer with Cu K<sub>α</sub> ( $\lambda$  = 0.154 nm) radiation. All yields refer to isolated products after purification by recrystallization.  $\gamma$ -Fe<sub>2</sub>O<sub>3</sub>@TiO<sub>2</sub>-EG-Cu(II) nanoparticles were prepared using a method previously reported in the literature.<sup>[41a]</sup>

### 2.2 | Typical procedure for preparation of 2,4,5-Triphenyl-1H-imidazole (3a)

$\gamma$ -Fe<sub>2</sub>O<sub>3</sub>@TiO<sub>2</sub>-EG-Cu(II) nanoparticles (2.5 mol%, 0.030 g) were added to a mixture of benzil (1 mmol, 0.210 g), benzaldehyde (1 mmol, 0.106 g) and NH<sub>4</sub>OAc (2.5 mmol, 0.192 g). The resulting mixture was stirred at 100 °C under neat conditions, until the reaction was judged to be complete by TLC (eluent = *n*-hexane–ethyl acetate, 7:3). After cooling to room temperature, hot ethanol (5 ml) was added to the reaction mixture and the catalyst was separated from the solution using an

external magnet, washed with ethanol ( $2 \times 10$  ml) and air-dried to be ready for the next run. Thereafter, the resultant mixture was concentrated under rotary vacuum evaporation and the obtained crude product was recrystallized from ethanol to afford the pure 2,4,5-triphenyl-1*H*-imidazole (0.290 g, 98%).

### 2.3 | Typical procedure for preparation of 1,2,4,5-Tetraphenylimidazole (3 t)

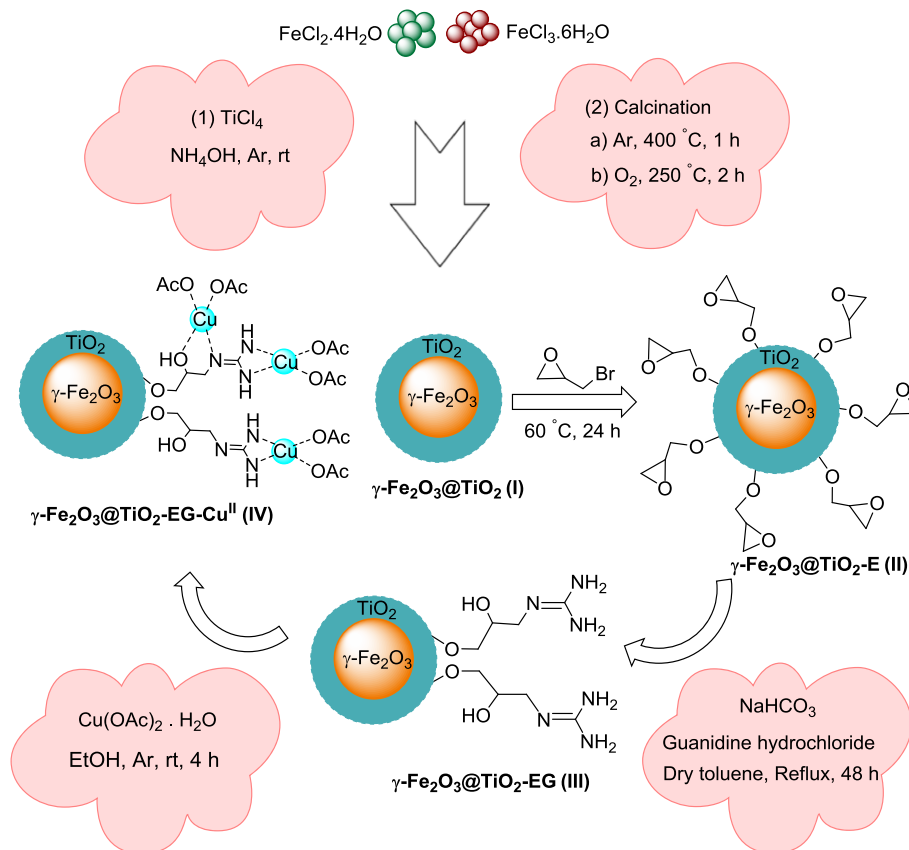
$\gamma\text{-Fe}_2\text{O}_3@TiO_2\text{-EG-Cu(II)}$  nanoparticles (2.5 mol%, 0.030 g,) were added to a mixture of benzil (1 mmol, 0.210 g), benzaldehyde (1 mmol, 0.106 g),  $\text{NH}_4\text{OAc}$  (1.5 mmol, 0.115 g) and aniline (1 mmol, 0.093 g). The resulting mixture was stirred at 100 °C under neat conditions, until the reaction was judged to be complete by TLC (eluent = *n*-hexane–ethyl acetate, 7:3). After cooling to room temperature, hot ethanol (5 ml) was added to the reaction mixture and the catalyst was separated from the solution using an external magnet, washed with ethanol ( $2 \times 10$  ml) and air-dried to be ready for the next run. Afterwards, the resultant mixture was concentrated under rotary vacuum evaporation and the

obtained crude product was recrystallized from ethanol to afford pure 1,2,4,5-tetraphenylimidazole (0.364 g, 98%).

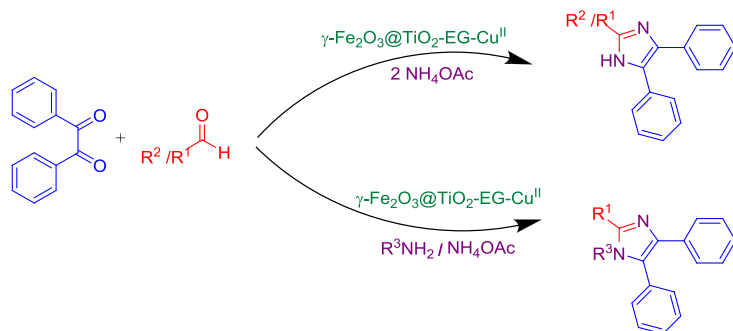
## 3 | RESULTS AND DISCUSSION

Nanomagnetic catalysts have received a great deal of attention in organic chemistry due to their easy separation from reaction mixtures using an external magnet (which is not time-consuming in comparison with the standard methods), clean forward reactions, and their having remarkable physical and chemical properties by controlling particle size and surface area. Recently, we successfully synthesized  $\gamma\text{-Fe}_2\text{O}_3@TiO_2\text{-EG-Cu(II)}$  as a novel and magnetically recyclable heterogeneous nanocatalyst<sup>[41a]</sup> (Scheme 1). The catalytic activity of the synthesized nanocatalyst was initially investigated in the one-pot synthesis of 1,4-disubstituted 1,2,3-triazoles, through alkyne–azide cycloaddition reactions, in water.<sup>[41a]</sup>

In the present study we decided to extend the application of  $\gamma\text{-Fe}_2\text{O}_3@TiO_2\text{-EG-Cu(II)}$  as a reusable solid acid nanomagnetic catalyst towards the efficient synthesis of 2,4,5-trisubstituted and 1,2,4,5-



**SCHEME 1** Overview of  $\gamma\text{-Fe}_2\text{O}_3@TiO_2\text{-EG-Cu(II)}$  preparation



R<sup>1</sup>: C<sub>6</sub>H<sub>5</sub>; 4-NO<sub>2</sub>C<sub>6</sub>H<sub>4</sub>; 4-CNC<sub>6</sub>H<sub>4</sub>; 4-FC<sub>6</sub>H<sub>4</sub>; 4-ClC<sub>6</sub>H<sub>4</sub>; 2-ClC<sub>6</sub>H<sub>4</sub>; 3-BrC<sub>6</sub>H<sub>4</sub>; 4-MeOC<sub>6</sub>H<sub>4</sub>; 2-MeOC<sub>6</sub>H<sub>4</sub>; 4-MeC<sub>6</sub>H<sub>4</sub>; 2-MeC<sub>6</sub>H<sub>4</sub>; 4-OHC<sub>6</sub>H<sub>4</sub>; 2-OHC<sub>6</sub>H<sub>4</sub>; 4-*ipr*C<sub>6</sub>H<sub>4</sub>; 4-(CH<sub>3</sub>)<sub>2</sub>NC<sub>6</sub>H<sub>4</sub>; C<sub>4</sub>H<sub>4</sub>N; 2-C<sub>4</sub>H<sub>3</sub>S

R<sup>2</sup>: C<sub>5</sub>H<sub>11</sub>; C<sub>6</sub>H<sub>13</sub>

R<sup>3</sup>: C<sub>6</sub>H<sub>5</sub>; 4-ClC<sub>6</sub>H<sub>4</sub>; 4-MeC<sub>6</sub>H<sub>4</sub>; 4-MeOC<sub>6</sub>H<sub>4</sub>; CH<sub>2</sub>C<sub>6</sub>H<sub>5</sub>

**SCHEME 2** Synthesis of 2,4,5-trisubstituted and 1,2,4,5-tetrasubstituted imidazoles *via* one-pot condensation reactions of aldehydes with benzil and ammonium acetate or ammonium acetate and amines in the presence of γ-Fe<sub>2</sub>O<sub>3</sub>@TiO<sub>2</sub>-EG-Cu(II)

tetrasubstituted imidazoles *via* one-pot condensation reactions of aldehydes with benzil and ammonium acetate or ammonium acetate and amines (Scheme 2).

### 3.1 | Characterization of γ-Fe<sub>2</sub>O<sub>3</sub>@TiO<sub>2</sub>-EG-Cu(II)

The γ-Fe<sub>2</sub>O<sub>3</sub>@TiO<sub>2</sub>-EG-Cu(II) catalyst synthesized based on the pathway described in Scheme 1 was then fully characterized using various techniques including FT-IR spectroscopy, powder XRD, HRTEM, TGA/DTG, EDS, VSM, ICP analysis and elemental analysis (CHNS).

FT-IR spectroscopy was engaged to compare the synthesized γ-Fe<sub>2</sub>O<sub>3</sub>@TiO<sub>2</sub>, epibromohydrin-functionalized γ-Fe<sub>2</sub>O<sub>3</sub>@TiO<sub>2</sub>, guanidinated epibromohydrin-functionalized γ-Fe<sub>2</sub>O<sub>3</sub>@TiO<sub>2</sub> and γ-Fe<sub>2</sub>O<sub>3</sub>@TiO<sub>2</sub>-EG-Cu(II) (Figure 1). The characteristic absorption band related to the stretching vibration of Fe—O bond in γ-Fe<sub>2</sub>O<sub>3</sub> was present at about 571–698 cm<sup>-1</sup>,<sup>[42]</sup> which was covered by the broad absorption band of Ti—O in the TiO<sub>2</sub> lattice at 500–850 cm<sup>-1</sup>.<sup>[43]</sup> Also, the absorption band at 1619 cm<sup>-1</sup> and the broad band appearing at 3100–3500 cm<sup>-1</sup> were in turn associated with bending and stretching vibrations of the adsorbed water molecules and the surface-attached hydroxyl groups (Figure 1a).<sup>[44]</sup> Immobilization of the epoxy ring to γ-Fe<sub>2</sub>O<sub>3</sub>@TiO<sub>2</sub> framework was identified by the methylene C—H stretching and bending vibration bands appearing at around 2872–2923 and 1454 cm<sup>-1</sup>, respectively (Figure 1b).<sup>[45]</sup> Moreover, C—O—C vibrational stretching modes were visualized at 1112 cm<sup>-1</sup>. These findings indicated the successful grafting of epoxy rings to the γ-Fe<sub>2</sub>O<sub>3</sub>@TiO<sub>2</sub> surface. Evidence for the ring opening of epoxy with guanidine groups was the appearance of indicative bands at around 3378 and 1454 cm<sup>-1</sup>, which were related to N—H and C—N stretching vibrations, respectively (Figure 1c).<sup>[44c]</sup> After coordination with Cu(II), the

diagnostic absorption bands corresponding to Cu—N and Cu—O vibrations were observed at 428 and 450 cm<sup>-1</sup>, respectively.<sup>[41b]</sup> The respective bands were covered by stretching vibration modes of Fe—O and Ti—O bonds. Furthermore, —NH<sub>2</sub> and probably —OH stretching

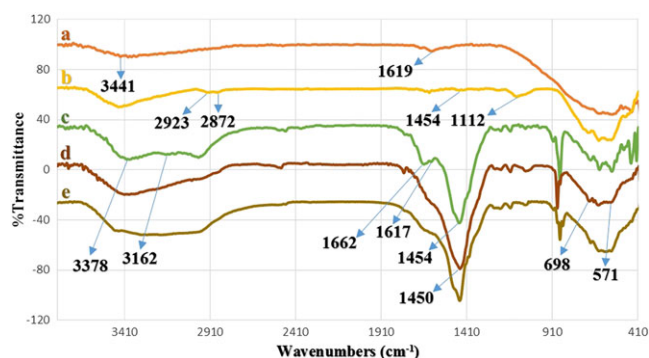


**FIGURE 1** FT-IR spectra of (a) γ-Fe<sub>2</sub>O<sub>3</sub>@TiO<sub>2</sub> nanoparticles, (b) epibromohydrin-functionalized γ-Fe<sub>2</sub>O<sub>3</sub>@TiO<sub>2</sub>-E, (c) guanidinated epibromohydrin-functionalized γ-Fe<sub>2</sub>O<sub>3</sub>@TiO<sub>2</sub>-EG, (d) γ-Fe<sub>2</sub>O<sub>3</sub>@TiO<sub>2</sub>-EG-Cu(II) and (e) γ-Fe<sub>2</sub>O<sub>3</sub>@TiO<sub>2</sub>-EG-Cu(II) recovered after sixth run

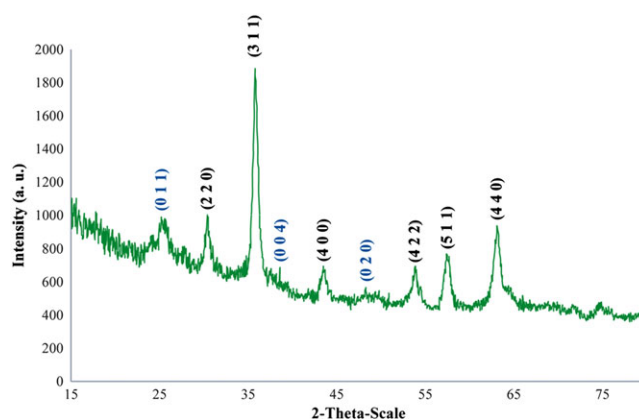


**FIGURE 2** XRD pattern of γ-Fe<sub>2</sub>O<sub>3</sub>@TiO<sub>2</sub>

frequencies (at around  $3162\text{--}3378\text{ cm}^{-1}$ ) were shifted to lower wavenumber as a result of the metallation process. In addition, NH and probably OH bending vibrations (positioned at  $1617$  and  $1619\text{ cm}^{-1}$ , respectively) were also shifted to lower frequencies after coordination with Cu(II). Likewise, C–N and C=N stretching vibrations (positioned at  $1454$  and  $1662\text{ cm}^{-1}$ ) were shifted to lower wavenumbers due to the metallation process (Figure 1d). On the other hand, bands at  $1634$  and  $1401\text{ cm}^{-1}$  in the spectrum of  $\gamma\text{-Fe}_2\text{O}_3\text{@TiO}_2\text{-EG-Cu(II)}$  were related to COO (in acetate),<sup>[42]</sup> which proved the presence of Cu in the catalyst. The mentioned absorption bands were covered by broad stretching vibration frequencies related to C–N bond. Accordingly, potent metal–ligand interaction was confirmed.

Powder XRD measurement was accomplished to identify the crystalline structure of  $\gamma\text{-Fe}_2\text{O}_3\text{@TiO}_2$ . As shown in Figure 2, the reflection planes of (2 2 0), (3 1 1), (4 0 0), (4 2 2), (5 1 1) and (4 4 0), which are ascribed to the cubic structure of  $\gamma\text{-Fe}_2\text{O}_3$  (JCPDS file

no. 04–0755), were readily recognized from the XRD pattern. Moreover, the existence of weak diffraction peaks relating to (0 1 1), (0 0 4) and (0 2 0) crystallographic faces could be assigned to anatase XRD diffraction peaks. Accordingly, the average crystallite sizes of  $\gamma\text{-Fe}_2\text{O}_3$  and  $\text{TiO}_2$  (anatase) which were calculated using the Debye–Scherrer equation were approximately 13 and 7 nm, respectively.

According to the HRTEM images of the catalyst (Figure 3), a relatively good monodispersity was obvious for the  $\gamma\text{-Fe}_2\text{O}_3\text{@TiO}_2\text{-EG-Cu(II)}$  structure. Interestingly, it is evident that a dark  $\gamma\text{-Fe}_2\text{O}_3$  core with an average size of about 10–20 nm was surrounded by a grey titania shell with a thickness of about 5–10 nm in the catalyst structure (Figure 3).

TGA/DTG study of  $\gamma\text{-Fe}_2\text{O}_3\text{@TiO}_2\text{-EG-Cu(II)}$  was conducted to investigate the thermal stability of the catalyst, as well as the amount of immobilized organic functional groups on the support (Figure 4). As can be seen in the TGA thermogram, the observed weight loss

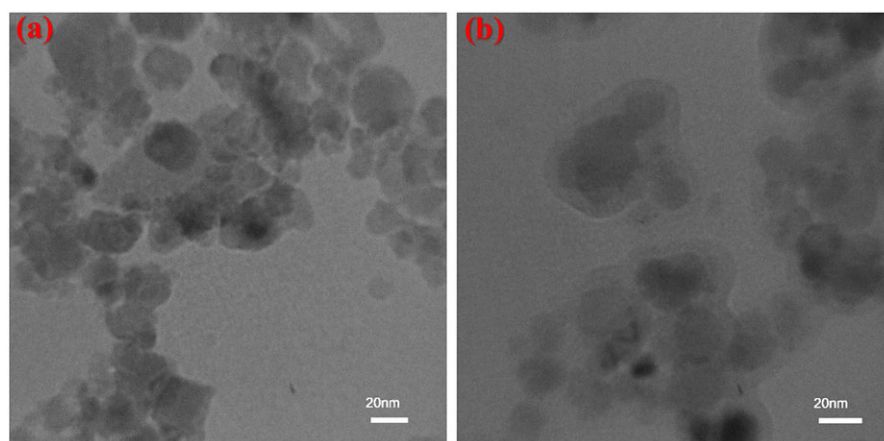


**FIGURE 3** HRTEM images of  $\gamma\text{-Fe}_2\text{O}_3\text{@TiO}_2\text{-EG-Cu(II)}$

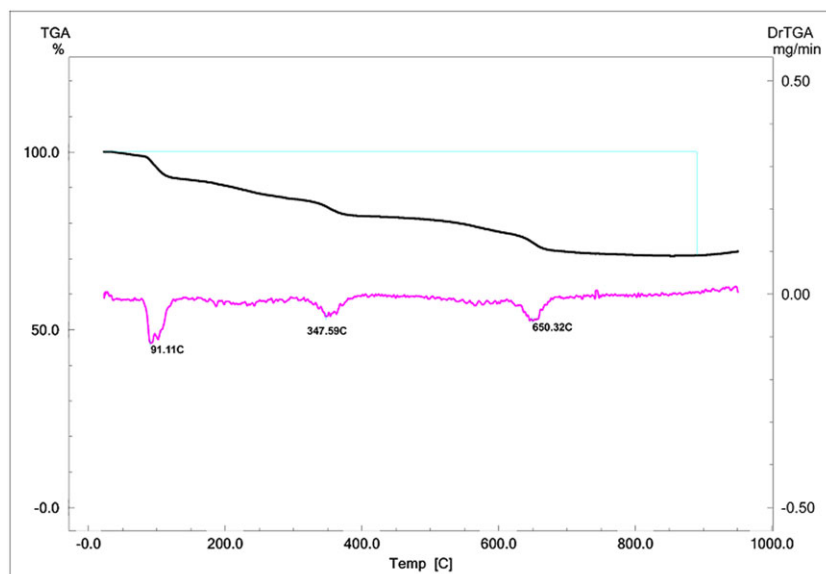


**FIGURE 4** TGA/DTG thermograms of  $\gamma\text{-Fe}_2\text{O}_3\text{@TiO}_2\text{-EG-Cu(II)}$

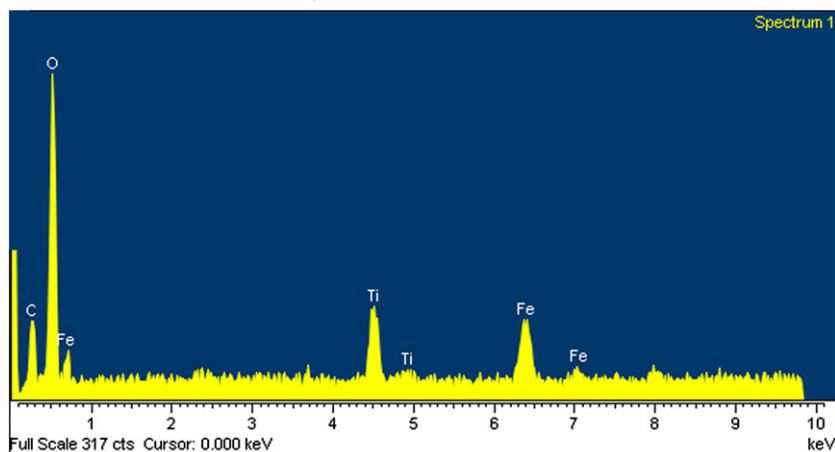


**FIGURE 5** EDS analysis of  $\gamma$ - $\text{Fe}_2\text{O}_3$ @ $\text{TiO}_2$ -EG-Cu(II)

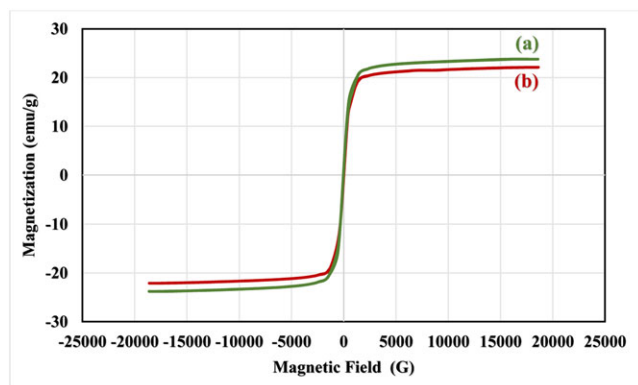


**FIGURE 6** Magnetization curves of (a)  $\gamma$ - $\text{Fe}_2\text{O}_3$ @ $\text{TiO}_2$  nanoparticles and (b)  $\gamma$ - $\text{Fe}_2\text{O}_3$ @ $\text{TiO}_2$ -EG-Cu(II)

at temperatures below 200 °C was related to the adsorbed water molecules on the support. Then, the decomposition of organic motifs occurred at temperatures ranging from 200 to 670 °C (17.23 wt%). Based on the TGA results, the amount of organic backbone supported on  $\gamma$ - $\text{Fe}_2\text{O}_3$ @ $\text{TiO}_2$  is estimated to be 0.70 mmol  $\text{g}^{-1}$ . These results were in a good agreement with the elemental analysis data ( $N = 3.01\%$  and  $C = 7.02\%$ ) and ICP analysis. The ICP analysis indicated that 0.74 mmol of copper was anchored on 1.00 g of the catalyst.

EDS analysis disclosed the existence of C, O, Fe, Ti and Cu elements (Figure 5). This analysis well demonstrated that Cu(II) is immobilized on the guanidinated epibromohydrin-functionalized  $\gamma$ - $\text{Fe}_2\text{O}_3$ @ $\text{TiO}_2$ .

The magnetic properties of  $\gamma$ - $\text{Fe}_2\text{O}_3$ @ $\text{TiO}_2$  and  $\gamma$ - $\text{Fe}_2\text{O}_3$ @ $\text{TiO}_2$ -EG-Cu(II) were measured at ambient temperature using VSM. As indicated in Figure 6, the saturation magnetization values for  $\gamma$ - $\text{Fe}_2\text{O}_3$ @ $\text{TiO}_2$  and  $\gamma$ - $\text{Fe}_2\text{O}_3$ @ $\text{TiO}_2$ -EG-Cu(II) were 23.79 and 22.12 emu  $\text{g}^{-1}$ , respectively. Indeed, the absence of hysteresis phenomenon indicated that both  $\gamma$ - $\text{Fe}_2\text{O}_3$ @ $\text{TiO}_2$  and  $\gamma$ -

$\text{Fe}_2\text{O}_3$ @ $\text{TiO}_2$ -EG-Cu(II) have superparamagnetism at room temperature. A slight decrease in the saturation magnetization of  $\gamma$ - $\text{Fe}_2\text{O}_3$ @ $\text{TiO}_2$  after the surface grafting could be attributed to the contribution of the non-magnetic materials.

### 3.2 | Catalytic synthesis of 2,4,5-Trisubstituted and 1,2,4,5-Tetrasubstituted Imidazoles in presence of $\gamma$ - $\text{Fe}_2\text{O}_3$ @ $\text{TiO}_2$ -EG-Cu(II)

To evaluate and optimize the catalytic behaviour of  $\gamma$ - $\text{Fe}_2\text{O}_3$ @ $\text{TiO}_2$ -EG-Cu(II) in the synthesis of imidazoles, initially a multicomponent condensation reaction for the preparation of 2,4,5-triphenyl-1*H*-imidazole was studied under various conditions (including different solvents, temperatures, amounts of catalyst and molar ratios of reactants). The results are summarized in Table 1. As a first step, to monitor whether the use of  $\gamma$ - $\text{Fe}_2\text{O}_3$ @ $\text{TiO}_2$ -EG-Cu(II) is crucial for this transformation, the multicomponent condensation reaction of benzil (1 mmol), benzaldehyde (1 mmol) and ammonium acetate (2.5 mmol) at 100 °C was conducted under solvent-free condition in the absence of  $\gamma$ - $\text{Fe}_2\text{O}_3$ @ $\text{TiO}_2$ -EG-Cu(II) and also in the presence of  $\gamma$ - $\text{Fe}_2\text{O}_3$ @ $\text{TiO}_2$ ,  $\gamma$ - $\text{Fe}_2\text{O}_3$ @ $\text{TiO}_2$ -E and  $\gamma$ - $\text{Fe}_2\text{O}_3$ @ $\text{TiO}_2$ -EG (Table 1, entries 1–4). The obtained results clearly indicate that  $\text{Fe}_2\text{O}_3$ @ $\text{TiO}_2$ -EG-Cu(II) is a vital catalyst for this condensation reaction (compare entry 5 with entries 1–4). It is interesting to note that temperature plays an important role in the catalytic synthesis of 2,4,5-triphenyl-1*H*-imidazole. To get more insight into the temperature effect, the model reaction was performed in the temperature range 90–120 °C. At 90 °C the reaction was completed in a prolonged time, while further increasing the reaction temperature (110 and 120 °C) had no great influence on the reaction rate (Table 1, entries 6–8). Hence, 100 °C was selected as the optimum temperature to accomplish

**TABLE 1** Optimization of various reaction parameters for one-pot synthesis of 2,4,5-triphenyl-1*H*-imidazole

Entry	Molar ratio of benzaldehyde:benzil: ammonium acetate	Catalyst (mol%)	Temperature (°C)	Solvent	Time (min)	Isolated yield (%)
1	1:1:2.5	—	100	—	60/24 (h)	0/0
2 <sup>a</sup>	1:1:2.5	0.03 (g)	100	—	60	Trace
3 <sup>b</sup>	1:1:2.5	0.03 (g)	100	—	60	Trace
4 <sup>c</sup>	1:1:2.5	0.03 (g)	100	—	60	Trace
<b>5</b>	<b>1:1:2.5</b>	<b>2.5</b>	<b>100</b>	—	<b>20</b>	<b>98</b>
6	1:1:2.5	2.5	110	—	20	98
7	1:1:2.5	2.5	120	—	20	98
8	1:1:2.5	2.5	90	—	30	98
9	1:1:2.5	1.6	100	—	25	90
10	1:1:2.5	3.2	100	—	20	98
11	1:1:2.5	4	100	—	20	98
12	1:1:2	2.5	100	—	30	96
13	1:1:3	2.5	100	—	20	98
14	1:1:3.5	2.5	100	—	20	98
15	1:1:2.5	2.5	Reflux	H <sub>2</sub> O	60	70
16	1:1:2.5	2.5	Reflux	EtOH	60	78
17	1:1:2.5	2.5	Reflux	CH <sub>3</sub> CN	60	73

<sup>a</sup>Reaction performed in the presence of  $\gamma$ -Fe<sub>2</sub>O<sub>3</sub>@TiO<sub>2</sub>.

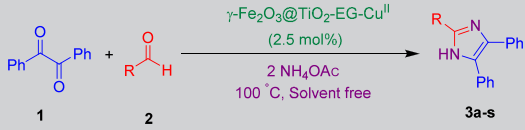
<sup>b</sup>Reaction performed in the presence of  $\gamma$ -Fe<sub>2</sub>O<sub>3</sub>@TiO<sub>2</sub>-E.

<sup>c</sup>Reaction performed in the presence of  $\gamma$ -Fe<sub>2</sub>O<sub>3</sub>@TiO<sub>2</sub>-EG.

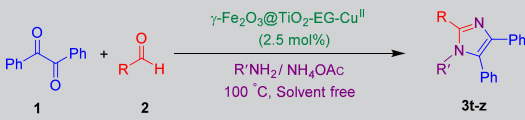
the reaction. To further develop the progress of reaction in terms of efficiency and time, the model reaction was carried out in the presence of various amounts of the catalyst. By applying lower catalytic amount (1.6 mol%), the product yield was found to be 90% in longer reaction time (Table 1, entry 9), whereas using higher amounts of catalyst (3.2 and 4 mol%) did not have any substantial effect on the reaction progress (Table 1, entries 10 and 11). To explore the effect of molar ratio of reactants on the reaction rate, we also implemented three separate experiments by applying 1:1:2, 1:1:3 and 1:1:3.5 molar ratios of benzaldehyde:benzil:ammonium acetate at 100 °C, under solvent-free condition (Table 1, entries 12–14). By using 1:1:2 molar ratio, the reaction rate was not so satisfactory. However, additional amounts of ammonium acetate did not have any noticeable influence on the reaction progress. Accordingly, the optimal molar ratio of benzaldehyde:benzil:ammonium acetate was selected as 1:1:2.5. To investigate the effect of solvent, the model reaction was carried out in H<sub>2</sub>O, EtOH and CH<sub>3</sub>CN (Table 1, entries 15–17). It was found that conducting the reaction under solvent-free condition generates the desired product in excellent yield within a short reaction time, in comparison with the use of solvent (compare entry 5 with entries 15–17).

After optimizing the reaction conditions, to show the general applicability of the present method, the reaction of benzil with a wide variety of aldehydes (aromatic, heteroaromatic and aliphatic) and ammonium acetate was investigated under the optimized conditions (Table 2). A broad range of aromatic aldehydes bearing both electron-donating and electron-withdrawing substituents underwent the successful one-pot, multicomponent cyclocondensation reactions to provide 2,4,5-trisubstituted imidazoles in excellent yields (Table 2, entries 1–15). Interestingly, heteroaromatic aldehydes as well as aliphatic aldehydes also afforded the corresponding imidazoles in high yields (Table 2, entries 16–19). In general, the aspect of this protocol is broad, since various functional groups were found to be compatible under such reaction conditions.

To widen the applicability of the present protocol, synthesis of 1,2,4,5-tetrasubstituted imidazoles was also investigated *via* the one-pot, multicomponent condensation reactions of benzil, aromatic aldehydes, ammonium acetate and a selection of primary aromatic amines, under the optimized conditions established for the preparation of 2,4,5-trisubstituted imidazoles (Table 3). As can be seen, electron-withdrawing substituents on aromatic ring of aldehyde and electron-donating substituents on

**TABLE 2** Synthesis of various 2,4,5-trisubstituted imidazoles in presence of  $\gamma\text{-Fe}_2\text{O}_3\text{@TiO}_2\text{-EG-Cu(II)}$  under solvent-free condition


Entry	R	Product	Time (min)	Isolated yield (%)
1	C <sub>6</sub> H <sub>5</sub>	<b>3a</b>	20	98
2	4-NO <sub>2</sub> C <sub>6</sub> H <sub>4</sub>	<b>3b</b>	25	95
3	4-CNC <sub>6</sub> H <sub>4</sub>	<b>3c</b>	25	95
4	4-FC <sub>6</sub> H <sub>4</sub>	<b>3d</b>	25	90
5	4-ClC <sub>6</sub> H <sub>4</sub>	<b>3e</b>	20	95
6	2-ClC <sub>6</sub> H <sub>4</sub>	<b>3f</b>	30	95
7	3-BrC <sub>6</sub> H <sub>4</sub>	<b>3 g</b>	30	95
8	4-MeOC <sub>6</sub> H <sub>4</sub>	<b>3 h</b>	30	90
9	2-MeOC <sub>6</sub> H <sub>4</sub>	<b>3i</b>	25	96
10	4-MeC <sub>6</sub> H <sub>4</sub>	<b>3j</b>	20	95
11	2-MeC <sub>6</sub> H <sub>4</sub>	<b>3 k</b>	20	98
12	4-OHC <sub>6</sub> H <sub>4</sub>	<b>3 l</b>	30	90
13	2-OHC <sub>6</sub> H <sub>4</sub>	<b>3 m</b>	25	92
14	4- <i>i</i> prC <sub>6</sub> H <sub>4</sub>	<b>3n</b>	30	91
15	4-(CH <sub>3</sub> ) <sub>2</sub> NC <sub>6</sub> H <sub>4</sub>	<b>3o</b>	30	85
16	C <sub>4</sub> H <sub>4</sub> N	<b>3p</b>	37	92
17	2-C <sub>4</sub> H <sub>3</sub> S	<b>3q</b>	20	90
18	C <sub>5</sub> H <sub>11</sub>	<b>3r</b>	25	95
19	C <sub>6</sub> H <sub>13</sub>	<b>3 s</b>	28	93

**TABLE 3** Synthesis of various 1,2,4,5-tetrasubstituted imidazoles in presence of  $\gamma\text{-Fe}_2\text{O}_3\text{@TiO}_2\text{-EG-Cu(II)}$  under solvent-free condition


Entry	R	R'	Product	Time (min)	Isolated yield (%)
1	C <sub>6</sub> H <sub>5</sub>	C <sub>6</sub> H <sub>5</sub>	<b>3 t</b>	25	98
2	4-ClC <sub>6</sub> H <sub>4</sub>	C <sub>6</sub> H <sub>5</sub>	<b>3u</b>	20	92
3	2-CH <sub>3</sub> OC <sub>6</sub> H <sub>4</sub>	C <sub>6</sub> H <sub>5</sub>	<b>3v</b>	27	94
4	C <sub>6</sub> H <sub>5</sub>	4-CH <sub>3</sub> C <sub>6</sub> H <sub>4</sub>	<b>3w</b>	18	90
5	C <sub>6</sub> H <sub>5</sub>	4-CH <sub>3</sub> OC <sub>6</sub> H <sub>4</sub>	<b>3x</b>	15	90
6	C <sub>6</sub> H <sub>5</sub>	4-ClC <sub>6</sub> H <sub>4</sub>	<b>3y</b>	28	90
7	C <sub>6</sub> H <sub>5</sub>	C <sub>6</sub> H <sub>5</sub> CH <sub>2</sub>	<b>3z</b>	23	92

aromatic ring of primary amines could almost equally accelerate the corresponding condensation reactions. Generally, the reactions were clean and no side products were detected. In all cases, the reactions proceeded

efficiently and gave the corresponding products in good to excellent yields within short reaction times.

In our experiments, the completion of the reaction is confirmed by the disappearance of aldehydes determined

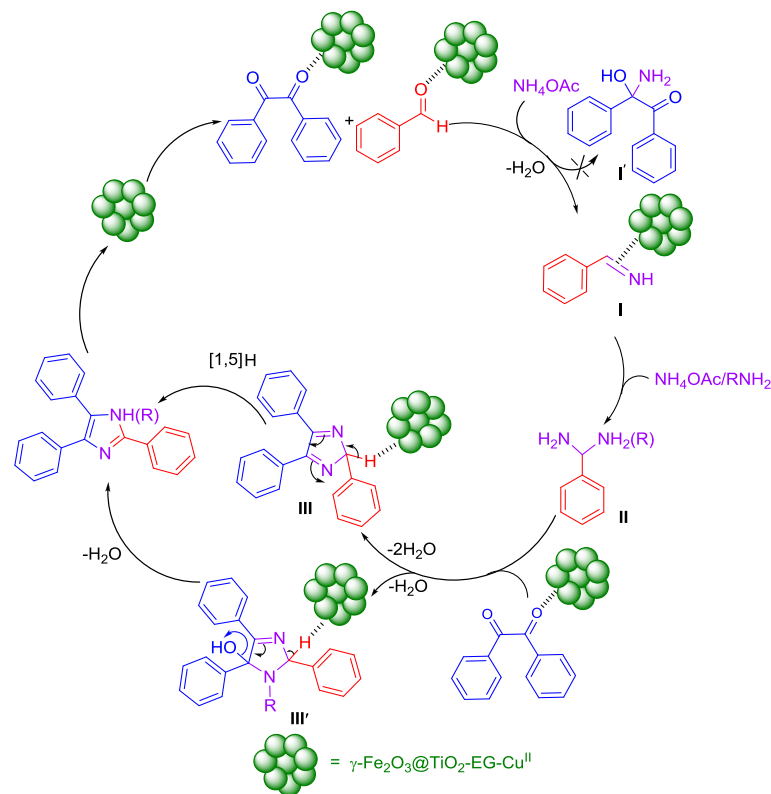


using TLC, followed by the appearance of a strong sharp absorption band in the FT-IR spectra of the products at around  $3338$  or  $1540\text{ cm}^{-1}$  and a medium absorption band at  $1666\text{ cm}^{-1}$ , which are assigned to N–H or C–N and C=N stretching vibrations of 2,4,5-trisubstituted imidazoles or 1,2,4,5-tetrasubstituted imidazoles, respectively. All of the obtained products were known and their physical data (colour, melting points) and spectral data (mass spectrometry) were found to be identical with those of authentic compounds. Selected compounds were further identified using FT-IR,  $^1\text{H}$  NMR and  $^{13}\text{C}$  NMR spectroscopies, the results of which were compared with literature data. A diagnostic  $^1\text{H}$  NMR signal at around  $12.70$ – $11.20$  ppm is assigned to the NH of 2,4,5-trisubstituted imidazoles. In  $^{13}\text{C}$  NMR spectra, a signal at around  $157.33$ – $144.04$  or  $150.71$ – $137.54$  ppm is allocated to C-2 of 2,4,5-trisubstituted imidazoles or 1,2,4,5-tetrasubstituted imidazoles, respectively. See the supporting information for details.

A postulated mechanism for this reaction is shown in Scheme 3. The crucial catalytic role of  $\gamma\text{-Fe}_2\text{O}_3@\text{TiO}_2\text{-EG-Cu(II)}$  in this condensation reaction was established by performing the reaction in the absence of  $\gamma\text{-Fe}_2\text{O}_3@\text{TiO}_2\text{-EG-Cu(II)}$ . In this context, even after a long reaction time, no product was obtained (Table 1, entry 1). It is speculated that the nucleophilic attack of the ammonia nitrogen (obtained from  $\text{NH}_4\text{OAc}$ ) on the activated carbonyl group of aldehyde results in formation of aryl

aldimine **I**. Subsequently, the catalyst facilitates the formation of intermediate **II**, by increasing the electrophilicity of the C=N on the aryl aldimine **I** towards the nucleophilic attack of ammonia or amine. There is no tendency between benzil and ammonia to produce  $\alpha$ -imino ketone **I'**. To understand which component (aldehyde or benzil) is more reactive toward ammonia, in two separate flasks,  $\text{NH}_4\text{OAc}$  was treated in turn with aldehyde and benzil under optimized reaction conditions, using stoichiometric amounts of the reactants. The rapid reaction of aldehyde with  $\text{NH}_4\text{OAc}$  produced aryl aldimine **I**, which next led to facile formation of intermediate **II** when treated with  $\text{NH}_4\text{OAc}$  or amine. On the other hand, a trace amount of  $\alpha$ -imino ketone **I'** was produced from the reaction of benzil with  $\text{NH}_4\text{OAc}$  or amine after a prolonged time. When the progress of the reaction mixture was followed precisely,  $\alpha$ -imino ketone **I'** was not detected. So, according to the above results, we can deduce that in the presence of aldehyde, nucleophilic attack of  $\text{NH}_4\text{OAc}$  or amine on benzil is not successful. Intermediate **II**, in the presence of  $\gamma\text{-Fe}_2\text{O}_3@\text{TiO}_2\text{-EG-Cu(II)}$ , condenses with benzil to form intermediate **III** or **III'** which in turn rearranges to 2,4,5-trisubstituted imidazole or 1,2,4,5-tetrasubstituted imidazole by a [1,5] hydrogen shift or dehydration, respectively, and then the re-generated catalyst re-enters the catalytic cycle.

The recovery and reusability of the catalyst were examined in the synthesis of 2,4,5-triphenyl-1*H*-



**SCHEME 3** Proposed mechanism for formation of 2,4,5-trisubstituted and 1,2,4,5-tetrasubstituted imidazoles in the presence of  $\gamma\text{-Fe}_2\text{O}_3@\text{TiO}_2\text{-EG-Cu(II)}$

imidazole. In this regard, after completion of the reaction, the reaction mixture was dissolved in hot ethanol and the catalyst was separated using an external magnet. Then the catalyst was washed with ethanol, air-dried and stored for subsequent reaction runs. The product was obtained in 98, 98, 97, 95, 92 and 89% isolated yields in six consecutive runs, which evidently indicated that the catalyst could be reused for at least six runs without loss of its activity (Figure 7).

It is important to note that the FT-IR spectrum of the nanocatalyst recovered after the sixth run (Figure 1e) indicated the entire preservation of the position, shape and relative intensity of the indicative absorption bands. These data verified that no substantial changes happened to the chemical structure of the functional groups and hydrogen bonding network of the nanocatalyst.

Also, it is noteworthy that the copper content of the freshly prepared catalyst which was obtained using ICP

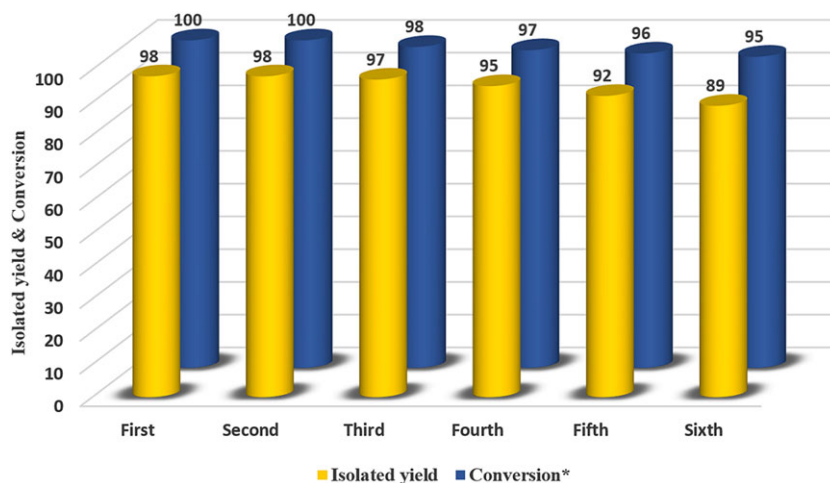


**FIGURE 7** Synthesis of 2,4,5-triphenyl-1*H*-imidazole in the presence of reused  $\gamma$ -Fe<sub>2</sub>O<sub>3</sub>@TiO<sub>2</sub>-EG-Cu(II). (\*data refer to conversion of benzaldehyde)

**TABLE 4** Comparison of catalytic activity of present catalyst with that of some other reported methods in preparation of 2,4,5-triphenyl-1*H*-imidazole and 1,2,4,5-tetraphenylimidazole

Entry <sup>a</sup>	Catalyst (loading)	Reaction conditions	Time (min)	Yield (%)
1	ZrO <sub>2</sub> - $\beta$ -CD <sup>b</sup> (40 mol%)	Solvent-free/100 °C	24	96 <sup>[46]</sup>
2	Yb (OTf) <sub>3</sub> (5 mol%)	HOAc/70 °C	120	95 <sup>[33]</sup>
3	Zinc(II) [tetra(4-methylphenyl)] (2 $\mu$ mol%)	EtOH/ultrasound/r.t.	70	94 <sup>[47]</sup>
4	L-Proline (15 mol%)	MeOH/reflux	540	90 <sup>[38]</sup>
5	Polymer-ZnCl <sub>2</sub> (0.102 g)	EtOH/reflux	240	96 <sup>[48]</sup>
6	Alum <sup>c</sup> (0.3 g)	EtOH/70 °C	150	93 <sup>[49]</sup>
7	InCl <sub>3</sub> .3H <sub>2</sub> O (10 mol%)	MeOH/r.t.	480	82 <sup>[19]</sup>
8	Silica sulfuric acid (0.5 g)	H <sub>2</sub> O/reflux	240	73 <sup>[30]</sup>
9	I <sub>2</sub> (5 mol%)	EtOH/75 °C	15	99 <sup>[23]</sup>
10	$\gamma$ -Fe <sub>2</sub> O <sub>3</sub> @TiO <sub>2</sub> -EG-Cu(II) (2.5 mol%)	Solvent-free/100 °C	15	98 (present study)
11	TiCl <sub>4</sub> .SiO <sub>2</sub> (50 mol%)	Solvent-free /110 °C	190	75 <sup>[50]</sup>
12	BF <sub>3</sub> .SiO <sub>2</sub> (0.32 g)	Solvent-free/140 °C	120	92 <sup>[51]</sup>
13	I <sub>2</sub> (10 mol%)	EtOH/75 °C	50	96 <sup>[52]</sup>
14	SBPPSA <sup>d</sup> (0.25 g)	Solvent-free/140 °C	60	90 <sup>[53]</sup>
15	PEG-400 (1.5 g)	PEG-400/110 °C	360	86 <sup>[54]</sup>
16	DABCO (0.7 mol%)	<i>t</i> -BuOH/60 °C	720–900	92 <sup>[35]</sup>
17	$\gamma$ -Fe <sub>2</sub> O <sub>3</sub> @TiO <sub>2</sub> -EG-Cu(II) (2.5 mol%)	Solvent-free/100 °C	20	98 (present study)

<sup>a</sup>Entries 1–10 refer to synthesis of 2,4,5-triphenyl-1*H*-imidazole. Entries 11–16 refer to synthesis of 1,2,4,5-tetraphenylimidazole.

<sup>b</sup>ZrO<sub>2</sub>-supported- $\beta$ -cyclodextrin.

<sup>c</sup>Potassium aluminium sulfate.

<sup>d</sup>Silica-bonded propylpiperazine-*N*-sulfamic acid.

analysis was 0.74 mmol of Cu per gram of the catalyst, while ICP analysis indicates that the catalyst after the sixth run comprises 0.68 mmol of Cu per gram. Fascinatingly, the amount of copper leached from the surface of the catalyst is very low.

To show the merits of the  $\gamma$ -Fe<sub>2</sub>O<sub>3</sub>@TiO<sub>2</sub>-EG-Cu(II) nanocatalyst over some catalysts previously reported in the literature, the catalytic performance of  $\gamma$ -Fe<sub>2</sub>O<sub>3</sub>@TiO<sub>2</sub>-EG-Cu(II) in the preparation of 2,4,5-triphenyl-1H-imidazole and 1,2,4,5-tetraphenyl-imidazole was compared with that of various reported catalysts (Table 4). As can be observed, although all of the protocols in Table 4 were able to produce good yields of desired products, some of them suffer from long reaction times to achieve such suitable yields (Table 4, entries 2–8, 11, 12 and 13–17) and the use of hazardous catalysts (Table 4, entries 9 and 13). However, the main drawbacks of almost all existing methods are difficult and tedious work-up procedures and most significantly none of them are magnetically recoverable. So, this comparison clearly indicates that the present protocol is better in terms of shorter reaction time and cleaner reaction media due to utilization of a green, nontoxic, nanomagnetic and eco-benign recyclable catalyst.

## 4 | CONCLUSIONS

In this research we attempted to expand the application of  $\gamma$ -Fe<sub>2</sub>O<sub>3</sub>@TiO<sub>2</sub>-EG-Cu(II) as an effective and environmentally benign nanomagnetic catalyst in organic reactions. In this sense, a new and efficient procedure for the preparation of 2,4,5-trisubstituted and 1,2,4,5-tetrasubstituted imidazoles under solvent-free condition is reported. Compared with traditional methods, the significant features of the current nanocatalyst in the reported approach are high yields of products, short reaction times, green reaction media, simple procedure, high atom economy and very wide range of substrates. Moreover, the presented catalytic system is non-volatile, non-explosive, easy to handle, thermally robust and must importantly magnetically recyclable for at least six cycles without any appreciable loss in its catalytic activity.

## ACKNOWLEDGEMENT

The authors gratefully acknowledge the partial support of this study by Ferdowsi University of Mashhad Research Council (grant no. 3/43955).

## ORCID

Batool Akhlaghinia  <http://orcid.org/0000-0002-9940-5045>

## REFERENCES

- [1] J. G. Lambardino, E. H. Wiseman, *J. Med. Chem.* **1979**, *17*, 1182.
- [2] T. N. Doman, S. L. McGovern, B. J. Witherbee, T. P. Kasten, R. Kurumbail, W. C. Stallings, D. T. Connolly, B. K. Shoichet, *J. Med. Chem.* **2002**, *45*, 2213.
- [3] T. Maier, R. Schmierer, K. Bauer, H. Bieringer, H. Buerstell, B. Sachse, US Patent 4820335, **1989**.
- [4] M. E. Pierce, D. J. Carini, G. F. Huhn, G. J. Wells, J. F. Arnett, *J. Org. Chem.* **1993**, *58*, 4642.
- [5] L. L. Chang, K. L. Sidler, M. A. Cascieri, S. Laszlo, G. Koch, B. Li, M. MacCoss, N. Mantlo, S. O'Keefe, M. Pang, A. Rolando, W. K. Hagmann, *Bioorg. Med. Chem. Lett.* **2001**, *11*, 2549.
- [6] T. F. Gallagher, S. M. Fier-Thompson, R. S. Garigipati, M. E. Sorenson, J. M. Smietana, D. Lee, P. E. Bender, J. C. Lee, J. T. Laydon, D. E. Griswold, M. C. Chabot-Fletcher, J. J. Breton, J. L. Adams, *Bioorg. Med. Chem. Lett.* **1995**, *5*, 1171.
- [7] P. Wasserscheid, W. Keim, *Angew. Chem. Int. Ed. Engl.* **2000**, *39*, 3772.
- [8] D. Bourissou, O. Guerret, F. P. Gabbai, G. Bertrand, *Chem. Rev.* **2000**, *100*, 39.
- [9] I. Satoru, Japn Kokkai Tokyo Koho JP 01, 117, 867, *Chem. Abstr.* **1989**, *111*, 214482.
- [10] a) H. Debus, *Eur. J. Org. Chem.* **1858**, *107*, 199. b) B. Radziszewski, *Eur. J. Inorg. Chem.* **1882**, *15*, 1493.
- [11] E. Kolvari, N. Koukabi, M. M. Hosseini, Z. Khandani, *RSC Adv.* **2015**, *5*, 3682.
- [12] S. Kantevari, S. V. N. Vuppapalapati, O. B. Dhanraj, L. Nagarapu, *J. Mol. Catal. A* **2007**, *266*, 109.
- [13] S. Balalaie, A. Arabanian, *Green Chem.* **2000**, *2*, 274.
- [14] A. R. Karimi, Z. Alimohammadi, M. M. Amini, *Molec. Divers.* **2010**, *14*, 635.
- [15] S. Rostamnia, E. Doustkhah, *Synlett* **2015**, *26*, 1345.
- [16] A. Teimouri, A. N. Chermahini, *J. Mol. Catal. A* **2011**, *346*, 39.
- [17] N. Aziizi, Z. Manochehri, A. Nahayi, S. Torkashvand, *J. Mol. Liq.* **2014**, *196*, 153.
- [18] Z. Zarnegar, J. Safari, *New J. Chem.* **2014**, *38*, 4555.
- [19] S. D. Sharma, P. Hazarika, D. Konwar, *Tetrahedron Lett.* **2008**, *49*, 2216.
- [20] M. M. Heravi, K. Bakhtiari, H. A. Oskooie, S. Taheri, *J. Mol. Catal. A* **2007**, *263*, 279.
- [21] L. Nagarapu, S. Apuri, S. Kantevari, *J. Mol. Catal. A* **2007**, *266*, 104.
- [22] A. R. Karimi, Z. Alimohammadi, J. Azizian, A. A. Mohammadi, M. R. Mohammadzadeh, *Catal. Commun.* **2006**, *7*, 728.
- [23] M. Kidwai, P. Mothsra, V. Bansal, R. K. Somvanshi, A. S. Ethayathulla, S. Dey, T. P. Singh, *J. Mol. Catal. A* **2007**, *265*, 177.
- [24] M. M. Heravi, F. Derikvand, F. F. Bamoharram, *J. Mol. Catal. A* **2007**, *263*, 112.
- [25] A. Y. Usyatinsky, Y. L. Khemelnitsky, *Tetrahedron Lett.* **2000**, *41*, 5031.
- [26] F. H. Seyede, A. N. Seyede, B. Zahra, *Monatsh. Chem.* **2012**, *144*, 387.

- [27] F. Xu, N. Wang, Y. Tian, G. Li, *J. Heterocycl. Chem.* **2013**, *50*, 668.
- [28] G. Sharma, Y. Jyothi, P. Lakshmi, *Synth. Commun.* **2006**, *36*, 2991.
- [29] S. Sarshar, D. Siev, M. M. Mjalli, *Tetrahedron Lett.* **1996**, *37*, 835.
- [30] A. Shaabani, A. Rahmati, *J. Mol. Catal. A* **2006**, *249*, 246.
- [31] J. N. Sngshetti, N. D. Kokare, S. A. Kotharkara, D. B. Shinde, *J. Chem. Sci.* **2008**, *120*, 463.
- [32] D. Song, C. Liu, S. Zhang, G. Luo, *Synth. React. Inorg. Met.-Org. Chem.* **2010**, *40*, 145.
- [33] L. M. Wang, Y. H. Wang, H. Tian, Y. F. Yao, J. H. Shao, B. Liu, *J. Fluorine Chem.* **2006**, *127*, 1570.
- [34] A. Maleki, R. Paydar, *RSC Adv.* **2015**, *5*, 33177.
- [35] S. N. Murthy, B. Madhav, Y. V. D. Nageswar, *Tetrahedron Lett.* **2010**, *51*, 5252.
- [36] M. M. Heravi, F. Derikv, M. Haghighi, *Monatsh. Chem.* **2008**, *139*, 31.
- [37] C. Mukhopadhyay, P. K. Tapaswi, M. G. B. Drew, *Tetrahedron Lett.* **2010**, *51*, 3944.
- [38] S. Samai, G. C. Nandi, P. Singh, M. S. Singh, *Tetrahedron Lett.* **2009**, *65*, 10155.
- [39] R. H. Shoar, G. Rahimzadeh, F. Derikvand, M. Farzaneh, *Synth. Commun.* **2010**, *40*, 1270.
- [40] A. Hasaninejad, A. Zare, M. Shekouhy, J. Ameri Rad, *J. Comb. Chem.* **2010**, *12*, 844.
- [41] a) R. Jahanshahi, B. Akhlaghinia, *RSC Adv.* **2016**, *6*, 29210. b) N. Razavi, B. Akhlaghinia, *RSC Adv.* **2015**, *5*, 12372. c) S. S. E. Ghodsinia, B. Akhlaghinia, *RSC Adv.* **2015**, *5*, 49849. d) R. Jahanshahi, B. Akhlaghinia, *RSC Adv.* **2015**, *5*, 104087. e) M. Zarghani, B. Akhlaghinia, *Appl. Organometal. Chem.* **2015**, *29*, 683. f) M. Zarghani, B. Akhlaghinia, *RSC Adv.* **2015**, *5*, 87769. g) Z. Zareie, B. Akhlaghinia, *Chem. Pap.* **2015**, *69*, 1421. h) M. Zarghani, B. Akhlaghinia, *RSC Adv.* **2016**, *6*, 31850. i) N. Razavi, B. Akhlaghinia, *New J. Chem.* **2016**, *40*, 447. j) N. Yousefi Siavashi, B. Akhlaghinia, M. Zarghani, *Res. Chem. Intermed.* **2016**, *42*, 5789. k) S. S. E. Ghodsinia, B. Akhlaghinia, R. Jahanshahi, *RSC Adv.* **2016**, *6*, 63613. l) Z. Zarei, B. Akhlaghinia, *RSC Adv.* **2016**, *6*, 106473. m) M. Zarghani, B. Akhlaghinia, *Bull. Chem. Soc. Jpn.* **2016**, *89*, 1192. n) R. Jahanshahi, B. Akhlaghinia, *Chem. Pap.* **2017**, *71*, 1351. o) N. Razavi, B. Akhlaghinia, R. Jahanshahi, *Catal. Lett.* **2017**, *147*, 360. p) M. Esmailpour, B. Akhlaghinia, R. Jahanshahi, *J. Chem. Sci.* **2017**, *129*, 313. q) S. M. Masjed, B. Akhlaghinia, M. Zarghani, N. Razavi, *Aust. J. Chem.* **2017**, *70*, 33. r) E. Karimian, B. Akhlaghinia, S. S. E. Ghodsinia, *J. Chem. Sci.* **2016**, *128*, 429. s) R. Jahanshahi, B. Akhlaghinia, *New J. Chem.* **2017**, *41*, 7203.
- [42] S. Sobhani, Z. Vahidi, Z. Zeraatkar, S. Khodadadi, *RSC Adv.* **2015**, *5*, 36552.
- [43] A. Banisharif, S. H. Elahi, A. F. Anaraki, A. A. Khodadadi, Y. Mortazavi, *IJNN* **2013**, *9*, 193.
- [44] a) Y. Gao, Y. Masuda, Z. Peng, T. Yonezawa, K. Koumoto, *J. Mater. Chem.* **2003**, *13*, 608. b) B. Klingenberg, M. A. Vannice, *Chem. Mater.* **1996**, *8*, 2755. c) A. Rostami, B. Atashkar, D. Moradi, *Appl. Catal. A* **2013**, *467*, 7.
- [45] F. Adam, K. M. Hello, H. Osman, *Chin. J. Chem.* **2010**, *28*, 2383.
- [46] Y. R. Girish, K. S. S. Kumar, K. N. Thimmaiah, K. S. Rangappa, S. Shashikanth, *RSC Adv.* **2015**, *5*, 75533.
- [47] J. Safari, S. D. Khalili, S. H. Banitaba, H. Dehghani, *J. Korean Chem. Soc.* **2011**, *55*, 1.
- [48] L. Wang, C. Cai, *Monatsh. Chem.* **2009**, *140*, 541.
- [49] A. A. Mohammadi, M. Mivechi, H. Kefayati, *Monatsh. Chem.* **2008**, *139*, 935.
- [50] B. F. Mirjalili, A. H. Bamoniri, L. Zamani, *Sci. Iran.* **2012**, *19*, 565.
- [51] B. Sadeghi, B. B. F. Mirjalili, M. M. Hashemi, *Tetrahedron Lett.* **2008**, *49*, 2575.
- [52] M. Kidwai, P. Mothra, *Tetrahedron Lett.* **2006**, *47*, 5029.
- [53] K. Niknam, A. Deris, F. Naeimi, F. Majleci, *Tetrahedron Lett.* **2011**, *52*, 4642.
- [54] X. C. Wang, H. P. Gong, Z. J. Quan, L. Li, H. L. Ye, *Chin. Chem. Lett.* **2009**, *20*, 44.

## SUPPORTING INFORMATION

Additional Supporting Information may be found online in the supporting information tab for this article.

**How to cite this article:** Nejatianfar M, Akhlaghinia B, Jahanshahi R. Cu(II) immobilized on guanidinated epibromohydrin-functionalized  $\gamma$ -Fe<sub>2</sub>O<sub>3</sub>@TiO<sub>2</sub> ( $\gamma$ -Fe<sub>2</sub>O<sub>3</sub>@TiO<sub>2</sub>-EG-Cu(II)): A highly efficient magnetically separable heterogeneous nanocatalyst for one-pot synthesis of highly substituted imidazoles. *Appl Organometal Chem.* 2017;e4095. <https://doi.org/10.1002/aoc.4095>